Journal of Applied Polymer Science

Conformal electrodeposition of poly(phenylene oxide) on TiO_2 nanotube arrays with high performance for lithium ion battery

Jixiang Duan,[1] Hongying Hou,[1] Xianxi Liu,[2] Qishu Liao,[1] Song Liu,[1] Ruijin Meng,[1] Zhenliang Hao,[1] Yuan Yao[1]

[1]Faculty of Material Science and Engineering, Kunming University of Science and Technology, Kunming 650093, China
[2]Faculty of Mechanical and Electrical Engineering, Kunming University of Science and Technology, Kunming 650093, China
Correspondence to: H. Hou (E-mail: hhy@dicp.ac.cn or hongyinghou@kmust.edu.cn)

ABSTRACT: In order to improve electrochemical performances of lithium ion battery (LIB), electrochemical integration of the membrane with the electrode was accomplished by conformal electrodeposition of poly(phenylene oxide) (PPO) on three-dimensional (3D) oriented TiO_2 nanotube arrays (TiO_2NT). The as-synthesized PPO/TiO_2NT membrane/electrode was investigated in terms of AC impedance, XPS, SEM, EDX, galvanostatic charge/discharge, rate performance, and cycle stability. As expected, PPO was indeed combined with TiO_2NT via conformal electrodeposition; furthermore, the integrated PPO/TiO_2NT membrane/electrode delivered much better rate performance than the traditional membrane/electrode, mainly attributed to large area of membrane/electrode/electrolyte, short ionic diffusion paths and fast ionic transport. © 2016 Wiley Periodicals, Inc. J. Appl. Polym. Sci. **2016**, *133*, 43685.

KEYWORDS: conformal electrodeposition; lithium ion battery; membrane/electrode; phenol; TiO_2 nanotube arrays

Received 24 January 2016; accepted 21 March 2016
DOI: 10.1002/app.43685

INTRODUCTION

Although lithium ion battery (LIB) has been widely used in the portable electronic devices such as laptop computers and mobile phones since its successful commercialization in 1990s, it is still necessary to continuously pursue new improvements for the ever-increasing energy storage demands.[1] For example, with the rapid development of micro-electro-mechanical system, 3D micro battery with high capacity per package area represents one of the new developing trends of LIB. It is well known that nanomorphology can endow the electrode active materials with large specific surface area and high performances. For example, self-organized TiO_2 nanotube arrays (TiO_2NT) via facile anodization were considered as one potential alternative anode material for micro LIB due to large surface area, small volume change, low toxicity, high safety, and tight combination with Ti substrate.[2,3] In order to save the space and maintain high performances, it should be reasonably considered to maximize the contact area of the membrane/electrode as much as possible.

As one of the important components in LIB, a desired membrane separator between two electrodes should possess double functions of preventing from electronic contact between two electrodes, while allowing for the crossing of Li^+ as much as possible. Therefore, the membrane separator played a crucial role in the performance of LIB.[4–6] Currently, porous polyolefin membranes such as polyethylene (PE) were the most dominant separator for LIB owing to high chemical stability, mechanical strength, and thermal shutdown.[7] However, there were still some limitations to be overcome. Firstly, PE separator in LIB was usually placed between two electrodes for the membrane/electrode by physical stack, in which only the highest top of the electrode can contact the membrane separator and the resultant contact area of the membrane/electrode was small, especially for the uneven electrode with sags and crests such as TiO_2NT. Secondly, the thickness of PE separator was usually about 20 μm, which may result in large internal resistance of LIB.[8] Additionally, PE separator may not be fully wetted due to its nonpolar nature, which would also cause high ionic resistance of the membrane/electrode.[9] Therefore, some strategies such as surface grafting of functional groups and blending with inorganic particles have been proposed to deal with the issues as mentioned above.[10,11] These strategies can indeed improve the wettability or thermal stability of PE separator to some degree, but fail to maximize the contact area of the membrane/electrode.[12] Therefore, it was necessary to pursue better strategy to solve the issues as much as possible.

It was reported that some organic monomers can be electropolymerized on the surface of the electrode, achieving the

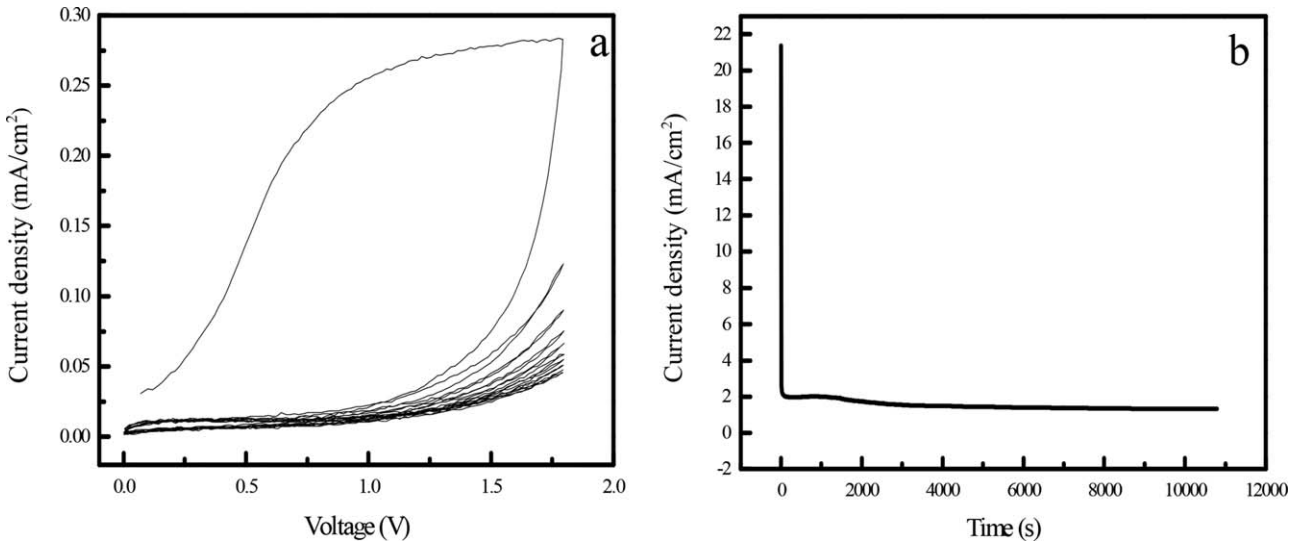

Figure 1. (a) CV curves and (b) chronoamperometry curve during the electropolymerization of phenol on TiO_2NT electrode.

conformal deposition of the membrane on the electrode. By this method, all the active surface areas of the electrode can contact the polymer separator.[13] Of course, the monomers with polar functional groups should be desirable for good wettability. Additionally, self-limiting electropolymerization was helpful for the nanoscale thickness of the polymer film. Seemingly, self-limiting electropolymerization of the insulating polar monomer should be preferable.

As reported elsewhere, the electropolymerization of phenol was self-limiting, and the resultant PPO film was usually less than 20 nm and exhibited desirable permeability.[14–17] Additionally, PPO film may be also wettable and compatible with liquid electrolytes due to the polar ether groups within its backbone. However, in most cases, PPO film via electropolymerization was usually applied in the fields such as the anti-corrosion of metal, the treatment of waster and the sensors, but seldom in LIB.

In this work, such efforts were made: conformal electrodeposition of PPO film on the surface of TiO_2NT for the membrane/electrode in LIB was designed and synthesized via one-step facile electropolymerization of phenol monomer. Furthermore, the as-synthesized PPO/TiO_2NT membrane/electrode was investigated in terms of AC impedance, XPS, SEM, EDX, galvanostatic charge/discharge, rate performance, and cycle stability.

EXPERIMENTAL

Preparation of PPO/TiO_2NT Membrane/Electrode

Firstly, TiO_2NT was prepared via facile anodization in a two-electrode cell, as reported in our previous work.[18] Electropolymerization of phenol was performed by CV and chronoamperometry in a three-electrode cell containing 0.02 M phenol and 0.1 M Na_2SO_4, where the as-prepared TiO_2NT was used as the working electrode, a saturated calomel electrode as the reference electrode, and Pt foil as the counter electrode, respectively. The software was controlled by an electrochemical workstation (Parstat4000, Princeton Applied Research, Oak Ridge, Tennessee, USA). *In situ* AC impedance was used to confirm the electropolymerization of phenol on TiO_2NT between 100 kHz to 0.01 Hz with 10 mV perturbation on the same electrochemical workstation. The active material can be removed by sonication for 3 d and the corresponding loading can be estimated according to the weight difference before and after sonication.

Characterization of Microstructure and Morphology

XPS spectrum of the sample was collected on X-ray photoelectron spectroscopy (PHI5000 Versaprobe-II, Japan) with Al Kα X-ray at 15 kV. The morphology of the sample was probed by scanning electron microscope (SEM, VEGA3 SBH Tescan) and the corresponding chemical composition was characterized by energy dispersive X-ray spectroscopy (EDX, Oxford Instruments X-ray Microanalysis 1350).

Electrochemical Measurements

The electrochemical performances of PPO/TiO_2NT membrane/electrode were investigated by assembling CR2025 coin cell with lithium foil as the counter electrode and reference electrode, in which porous nonwoven fabric was used as the separator, and the electrolyte was 1 M $LiPF_6$ in ethylene carbonate/diethyl carbonate (1:1 in volume). The coin cell was assembled in an argon-filled glove box (Mikrouna Super 1220/750/900) with the levels of O_2 and H_2O less than 0.1 ppm. The cell was measured by galvanostatic charge/discharge between 0.1 and 3.0 V (vs Li/Li^+) on Neware battery testing system (CT-3008W) at room temperature. The charge/discharge rates were at 0.3 C, 2.4 C, 4.8 C, 9.6 C, 15 C, 18 C and 25 C, respectively. For comparison, TiO_2NT with PE membrane (PE/TiO_2NT) via physical stack was investigated under the same conditions.

RESULTS AND DISCUSSION

Electropolymerization of Phenol on TiO_2NT Electrode

The electropolymerization of phenol monomer on TiO_2NT electrode can be performed via CV or chronoamperometry, as shown in Figure 1. Obviously, during the first positive scanning, a well-defined current peak at about 1.5 V was visible in Figure 1(a), corresponding to the electro-oxidation of phenol on TiO_2NT electrode; during negative CV scanning, no reductive current density peak can be observed, implying that the electro-

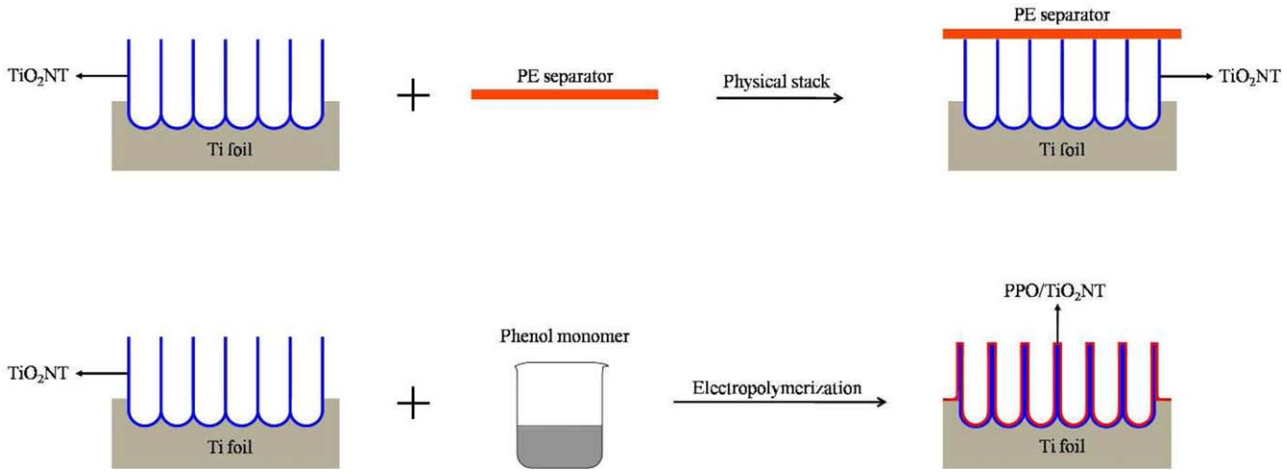

Figure 2. Schematic diagram of the fabrication procedures of PE/TiO_2NT membrane/electrode and PPO/TiO_2NT membrane/electrode. [Color figure can be viewed in the online issue, which is available at wileyonlinelibrary.com.]

oxidation of phenol was irreversible. In the second cycle, this current density peak became weaker, indicating the passivation of TiO_2NT electrode due to conformal electrodeposition of the insulating PPO film. This phenomenon became more and more significant with the increase of the cycle number.

Based on CV curves, the electropolymerization of phenol was also performed via chronoamperometry at 1.5 V, as shown in Figure 1(b). After an initial abrupt fall, the current density gradually decreased till to 3 h due to the gradual passivation of TiO_2NT electrode and slow increase of the internal resistance, indicating the formation of self-limiting PPO film on TiO_2NT electrode.

The fabrication procedures of traditional PE/TiO_2NT membrane/electrode and PPO/TiO_2NT membrane/electrode were schemed in Figure 2. In the case of conventional PE/TiO_2NT membrane/electrode, PE membrane was physically stacked with TiO_2NT, resulting in small contact area of the resultant membrane/electrode; to be different, PPO film was conformally electrodeposited on the surface of TiO_2NT electrode via electropolymerization of phenol monomer, maximizing the contact area as much as possible. The conformal configuration of PPO/TiO_2NT can allow for easier access of Li^+ to the entire surface of the hollow TiO_2 nanotubes. Additionally, the thickness of the conformal PPO film was also far less than that of the former, facilitating to reduce the internal resistance of LIB.

According to generally accepted electropolymerization mechanism of phenol in Scheme 1,[19] the anodic reaction occurred through one-electron transfer to phenol, accompanied with the formation of the aromatic free radicals. Then, these aromatic free radicals underwent C-O coupling for the dimers, while limiting the direct oxidation reaction from phenol to quinine.[20] The resulting dimers can be further oxidized for the polymer with high molecular weight after the following steps.

In situ AC impedance spectroscopy was used to confirm the effectiveness of electrodeposition of PPO on TiO_2NT electrode by monitoring the internal resistance of TiO_2NT electrode before and after electropolymerization, in Figure 3. As shown in Figure 3(a), the oblique line at low frequency after electropolymerization was higher than before, implying better electrochemical behaviors of PPO/TiO_2NT membrane/electrode. Additionally, after electropolymerization, the internal resistance of PPO/TiO_2NT was larger than that of bare TiO_2NT electrode according to the intercept of Nyquist plots at high frequency with real axis in Figure 3(b), mainly attributed to the conformal electrodeposition of insulating PPO film on TiO_2NT electrode.

SEM-EDX

Figure 4 showed SEM images of TiO_2NT before and after electropolymerization. Clearly, before electropolymerization, TiO_2 did consist of many hollow ordered nanotubes vertical to the surface of Ti substrate with an outer diameter of 100~140 nm and a length of 1.2 μm, as shown in Figure 4(a). After electropolymerization, TiO_2NT was coated by thin conformal PPO film, as shown in Figure 4(b). Seemingly, the morphology and dimension of the nanotubes were still visible after conformal electrodeposition due to self-limiting electropolymerization of phenol, which can maintain large surface area and shorten the

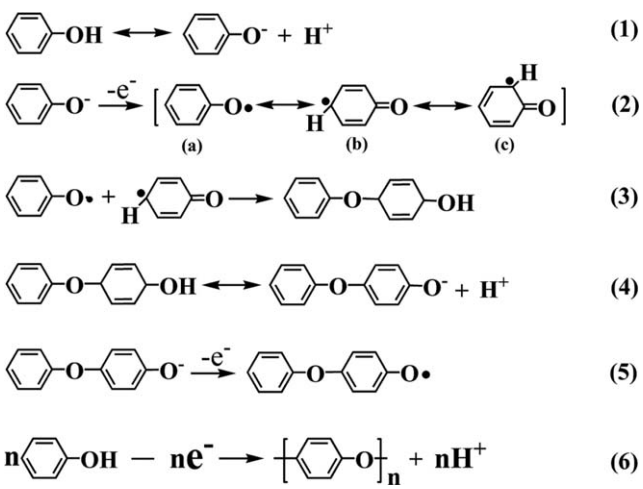

Scheme 1. The proposed electropolymerization mechanism of phenol monomer.[19]

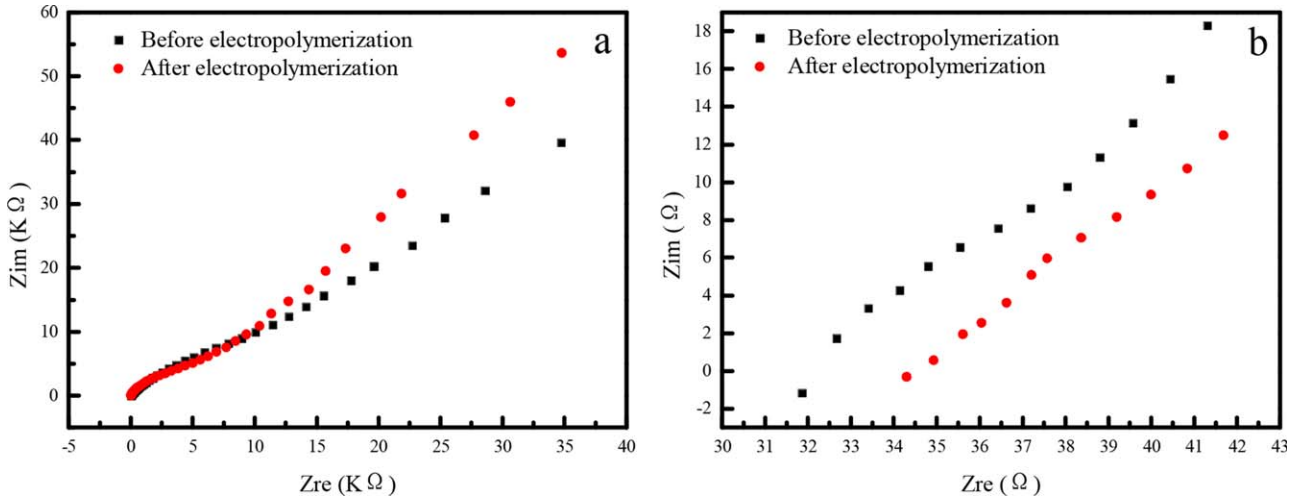

Figure 3. (a) Nyquist plots of TiO_2NT before and after electropolymerization of phenol; (b) zoomed in Nyquist plots at high frequency. [Color figure can be viewed in the online issue, which is available at wileyonlinelibrary.com.]

ionic/electronic diffusion path. EDX spectrum of PPO/TiO_2NT membrane/electrode was shown in Figure 4(c). As expected, several signals corresponding to Ti, O, C, and F elements were visible, in which the signal of F element may be caused by residual F^- during the preparation of TiO_2NT electrode. Of course, the signal of C element was due to conformal electrodeposition of PPO film on TiO_2NT electrode, while the signal of O element was from two sources of PPO film and TiO_2NT.

XPS

XPS technique was employed to further identify the chemical structure of PPO/TiO_2NT membrane/electrode. As shown in the wide scan XPS spectrum in Figure 5(a), several sharp peaks corresponding to Ti, O, and C elements were detected in PPO/TiO_2NT sample. In detail, two broad peaks at binding energy of about 458.6 eV and 464.2 eV were observed in Figure 5(b), corresponding to the characteristic Ti $2p_{1/2}$ and Ti $2p_{3/2}$ peaks of Ti^{4+}, respectively.[21] In Figure 5(c), two C 1s peaks centered at 284.7 eV and 285.8 eV can be attributed to C-C bonds and C-O ether bonds, corresponding to aromatic carbon and chain propagation within PPO, respectively, which was in agreement with electrodeposition of PPO on Pt or Fe electrode.[22,23] In Figure 5(d), O 1s core peak was composed of three main peaks at 531.0 eV (C-O), 529.8 eV (Ti-O) and 532.9 eV (O-H hydroxyl), corresponding to oxygen in PPO and TiO_2NT, respectively.[24–26]

Charge/Discharge Performances

Figure 6 showed the galvanostatic charge/discharge curves of PE/TiO_2NT and PPO/TiO_2NT membrane/electrodes. Li^+ insertion into and extraction from TiO_2NT follow the reversible chemical formula (7)[27]:

$$TiO_2 + xLi^+ + xe^- \leftrightarrow Li_xTiO_2 (0 \le x \le 1) \quad (7)$$

where x is the coefficient, corresponding to the amount of Li^+ insertion into and extraction from TiO_2 structure. A monotonic decrease in the voltage was observed during the first discharge, followed by a pseudo-plateau at about 1.1 V due to irreversible phase transition.[28,29] The initial discharge capacity of PE/TiO_2NT membrane/electrode was about 277 mAh/g, slightly lower than the theoretical capacity of 336 mAh/g ($x = 1$), while the initial discharge capacity of PPO/TiO_2NT membrane/electrode was about 347 mAh/g, higher than that of PE/TiO_2NT membrane/electrode and closer to theoretical value. Furthermore, the initial irreversible capacity loss of PPO/TiO_2NT membrane/electrode can be calculated to be 24% according to the

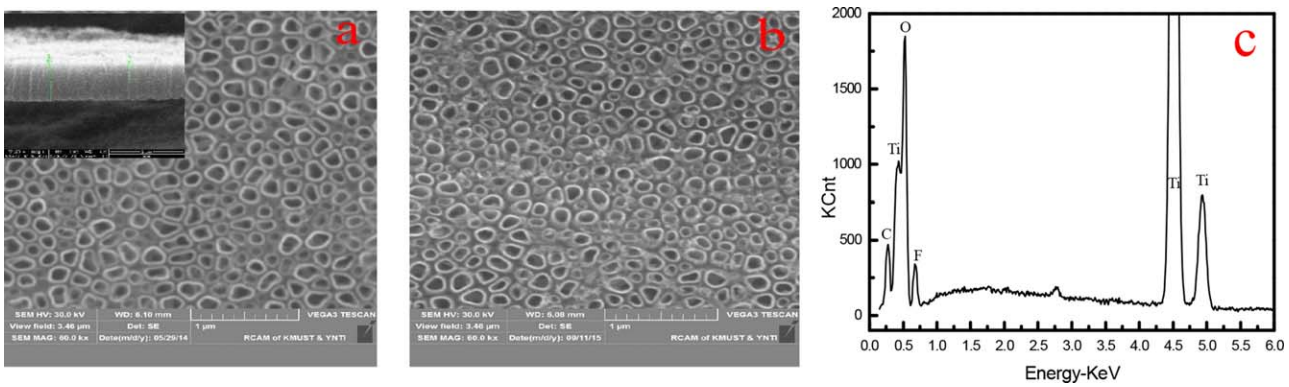

Figure 4. SEM images of (a) TiO_2NT (the inset: cross-section SEM image), (b) PPO/TiO_2NT, and (c) EDX spectrum of PPO/TiO_2NT. [Color figure can be viewed in the online issue, which is available at wileyonlinelibrary.com.]

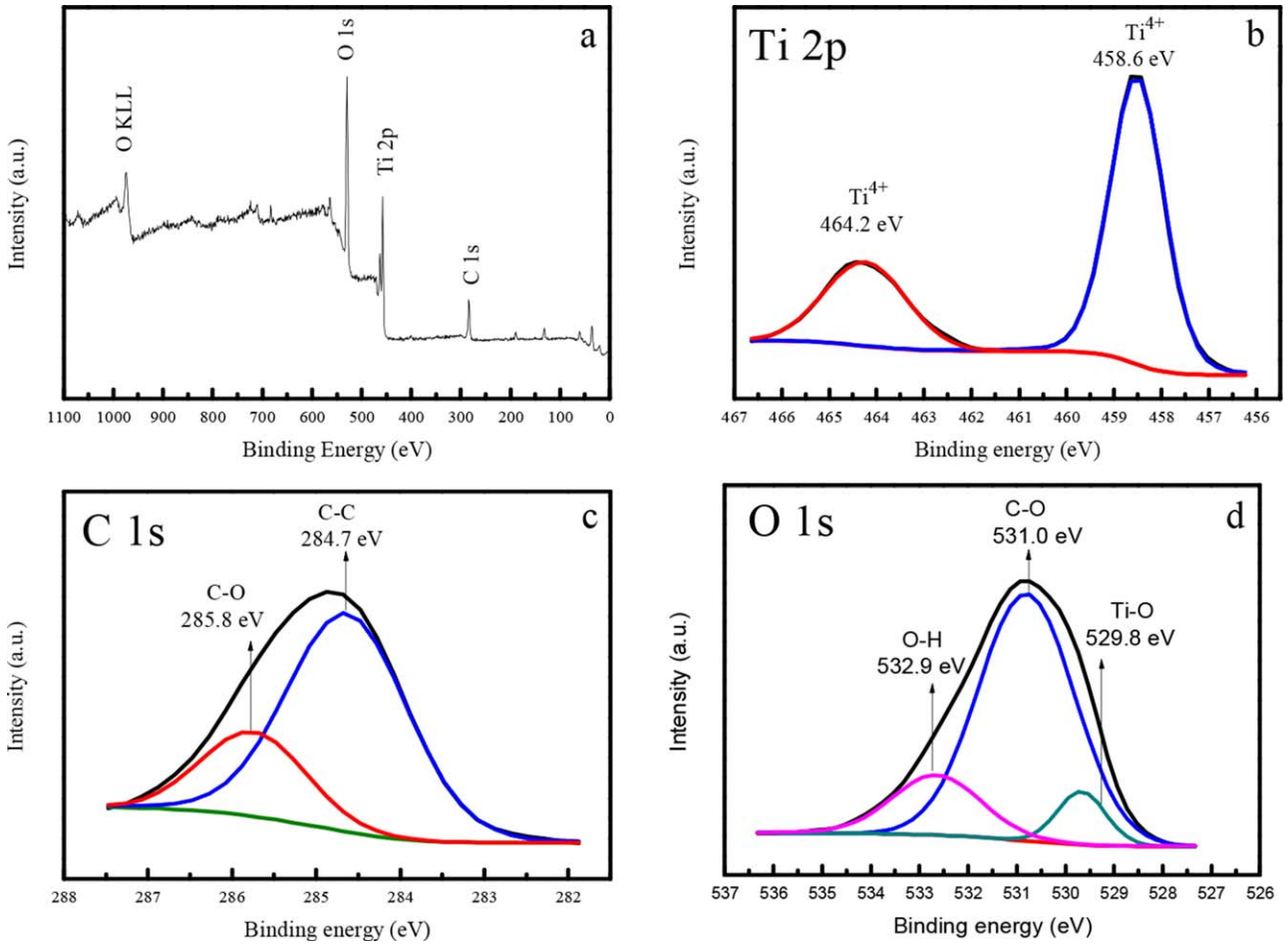

Figure 5. (a) Wide-scan XPS spectrum of PPO/TiO_2NT, XPS spectra of (b) Ti 2p, (c) C 1s, and (d) O 1s in PPO/TiO_2NT. [Color figure can be viewed in the online issue, which is available at wileyonlinelibrary.com.]

difference of first and second discharge capacity, lower than 44% of PE/TiO_2NT membrane/electrode.

Three possible reasons were responsible for the improved performances. Firstly, the conformal configuration of PPO/TiO_2NT membrane/electrode could maximize the contact area of the triple-phase membrane/electrode/electrolyte and thus accelerate the ionic transport.[13] Secondly, the thickness of PPO film via self-limiting electropolymerization of phenol was nanoscale,

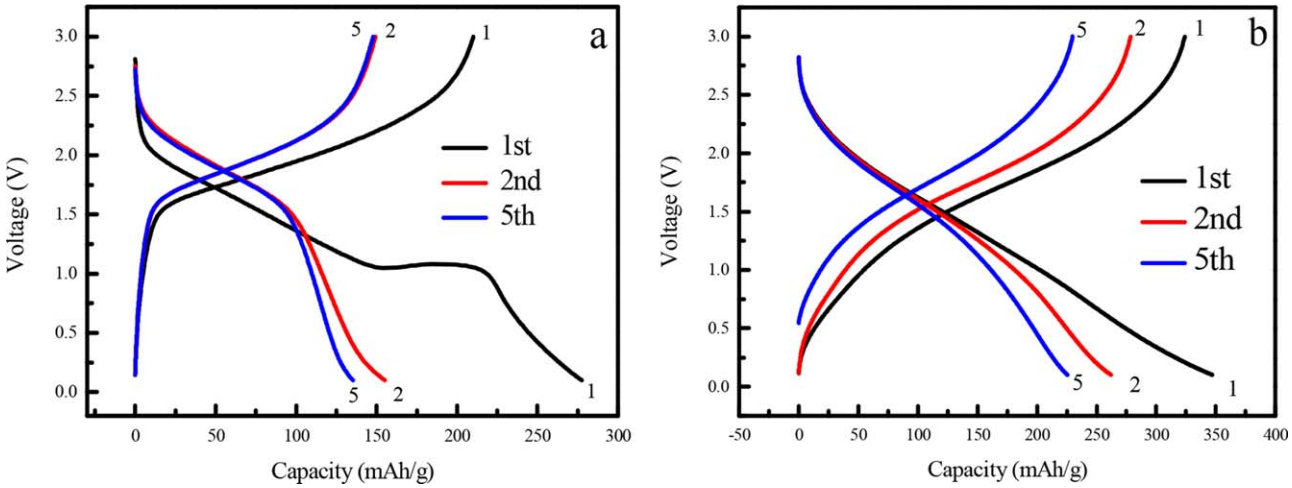

Figure 6. 1st, 2nd and 5th charge/discharge curves of (a) PE/TiO_2NT and (b) PPO/TiO_2NT at 0.3 C. [Color figure can be viewed in the online issue, which is available at wileyonlinelibrary.com.]

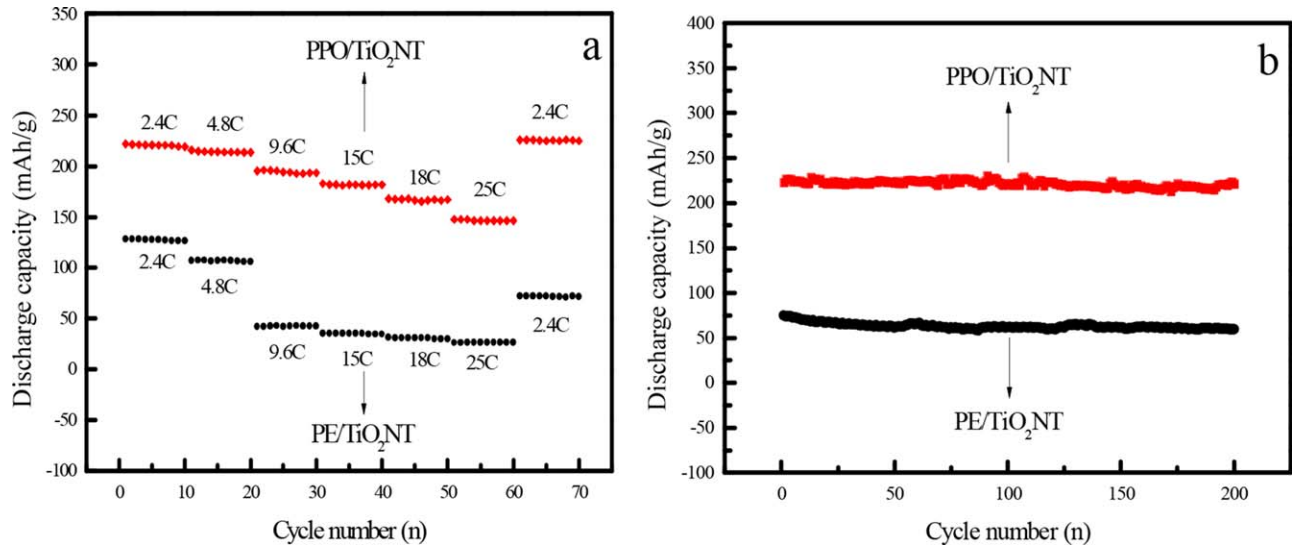

Figure 7. (a) The rate performances of PPO/TiO_2NT and PE/TiO_2NT at 2.4 C, 4.8 C, 9.6 C, 15 C, 18 C, and 25 C; (b) cycle stabilities of PPO/TiO_2NT and PE/TiO_2NT after high rate performances. [Color figure can be viewed in the online issue, which is available at wileyonlinelibrary.com.]

resulting in short Li^+ diffusion path and low internal resistance. Finally, the polar nature of PPO film can facilitate the wettability and compatibility with liquid electrolyte in LIB. Seemingly, the enhanced performances of PPO/TiO_2NT membrane/electrode can be attributed to the joint contributions of three factors.

Figure 7(a) showed the rate performances of both membrane/electrodes at 2.4 C, 4.8 C, 9.6 C, 15 C, 18 C and 25 C, and the corresponding discharge capacities were listed in Table I. Obviously, conformal PPO/TiO_2NT membrane/electrode displayed better discharge capacities than PE/TiO_2NT at all rates. For example, the discharge capacity of PPO/TiO_2NT membrane/electrode was as high as about 147 mAh/g even at 25 C, much higher than that of PE/TiO_2NT membrane/electrode. What's more, when the rate was set back to 2.4 C, the capacity of PPO/TiO_2NT membrane/electrode can immediately recover to the original level, while the capacity of PE/TiO_2NT membrane/electrode was only about 56% of the original value. It was reported that rapid ionic diffusion was necessary for high rate capacity.[27] Seemingly, the conformal PPO/TiO_2NT membrane/electrode can significantly improve the performance of LIB, especially at high rates. Additionally, the well-recoverable capacity of PPO/TiO_2NT membrane/electrode even after high rate discharge indicated higher structure stability and endurance to great change of the current than PE/TiO_2NT membrane/electrode.

Both membrane/electrodes were further cycled at 2.4 C for 200 cycles after the rate performances, as shown in Figure 7(b). It was noted that the discharge capacity of PPO/TiO_2NT membrane/electrode can be stably maintained at about 225 mAh/g, much higher than 70 mAh/g of PE/TiO_2NT membrane/electrode. The corresponding capacity retention of PPO/TiO_2NT membrane/electrode was about 100%, higher than 80% of PE/TiO_2NT membrane/electrode. Obviously, higher cycle stability even after high rate discharge was attributed to the maximized contact area of membrane/electrode/electrolyte, the minimized internal resistance and the accelerated electronic/ionic transport of PPO/TiO_2NT membrane/electrode.

CONCLUSIONS

PPO/TiO_2NT membrane/electrode was designed and synthesized via one-step conformal electrodeposition of PPO film on the surface of TiO_2NT electrode. As expected, the as-prepared conformal PPO/TiO_2NT membrane/electrode delivered much better electrochemical performances than PE/TiO_2NT membrane/electrode, especially at high rate. No doubt, the conformal electrodeposition of PPO film on 3D oriented TiO_2NT facilitated to maximize the contact area of membrane/electrode/electrolyte, to minimize the internal resistance and to accelerate the ionic transport, which jointly contributed into the modified electrochemical performances.

ACKNOWLEDGMENTS

This work was financially supported by the National Natural Science Foundation of China (grant number 51363011), the 46th Scientific Research Foundation for the Returned Overseas Chinese Scholars, State Education Ministry in China (6488-20130039), the Program of High-level Introduced Talent of Yunnan Province (10978125), and the Project of Key Discipline (14078232 and 14078311).

Table I. The Reversible Discharge Capacities of PE/TiO_2NT and PPO/TiO_2NT at Various Rates

Membrane/electrode	2.4 C	4.8 C	9.6 C	15 C	18 C	25 C	2.4 C
PE/TiO_2NT (mAh/g)	128	107	42	35	30	26	70
PPO/TiO_2NT (mAh/g)	221	215	194	182	167	147	225

REFERENCES

1. Goodenough, J.; Kyu-Sung, P. *J. Am. Chem. Soc.* **2013**, *135*, 1167.
2. Meng, R.; Hou, H.; Liu, X.; Yan, C.; Duan, J.; Liu, S. *Ceram. Int.* **2016**, *42*, 6039.
3. Plylahan, N.; Maria, S.; Phan, T.; Letiche, M.; Martinez, H.; Courreges, C.; Knauth, P.; Djenizian, T. *Nanoscale Res. Lett.* **2014**, *9*, 1.
4. Xiong, M.; Tang, H.; Wang, Y.; Lin, Y.; Sun, M.; Yin, Z.; Pan, M. *J. Power Sources* **2013**, *241*, 203.
5. Xu, K. *Chem. Rev.* **2004**, *35*, 4303.
6. Fu, D.; Luan, B.; Argue, S.; Bureau, M.; Davidson, I. *J. Power Sources* **2012**, *206*, 325.
7. Shi, J.; Fang, L.; Hao, L.; Hong, Z.; Zhu, B.; Zhu, L. *J. Membr. Sci.* **2013**, *437*, 160.
8. Gowda, S.; Reddy, A.; Shaijumon, M.; Zhan, X.; Ci, L.; Ajayan, P. *Nano Lett.* **2011**, *11*, 101.
9. Li, B.; Li, Y.; Dai, D.; Chang, K.; Tang, H.; Chang, Z.; Wang, C.; Yuan, X.; Wang, H. *ACS Appl. Mater. Interfaces.* **2015**, *7*, 20184.
10. Kim, K.; Kim, J.; Park, M.; Kwon, H.; Kim, H.; Kim, Y. *J. Power Sources* **2012**, *198*, 298.
11. Shi, C.; Zhang, P.; Chen, L.; Yang, P.; Zhao, J. *J. Power Sources* **2014**, *270*, 547.
12. Peng, K.; Wang, B.; Li, Y.; Ji, C. *RSC Adv.* **2015**, *5*, 81468.
13. Plylahan, N.; Letiche, M.; Barr, M.; Ellis, B.; Maria, S.; Pan, T.; Bloch, E.; Knauth, P.; Djenizian, T. *J. Power Sources* **2015**, *273*, 1182.
14. Deheryan, S.; Cott, D.; Muller, R.; Timmermans, M.; Heyns, M. *Carbon* **2015**, *88*, 42.
15. Tevi, T.; Yaghoubi, H.; Wang, J.; Takshi, A. *J. Power Sources* **2013**, *241*, 589.
16. Hou, H.; Vacandio, F.; Vona, M.; Knauth, P. *J. Appl. Polym. Sci.* **2013**, *129*, 1151.
17. Rhodes, C.; Long, J.; Doescher, M.; Fontanella, J.; Rolison, D. *J. Phys. Chem. B* **2004**, *108*, 13079.
18. Meng, R.; Hou, H.; Liu, X.; Hu, W.; Duan, J.; Liu, S. *Ceram. Int.* **2015**, *41*, 9988.
19. Bao, L.; Xiong, R.; Wei, G. *Electrochim. Acta* **2010**, *55*, 4030.
20. Hou, H.; Vacandio, F.; Vona, M.; Knauth, P. *Electrochim. Acta* **2012**, *81*, 58.
21. Zhou, H.; Zhang, Y. *J. Power Sources* **2013**, *239*, 128.
22. Rhodes, C.; Long, J.; Doescher, M.; Dening, B.; Rolison, D. *J. Non-Cryst. Solids* **2004**, *350*, 73.
23. Lapuente, R.; Quijada, C.; Huerta, F.; Cases, F.; Vazquez, J. *Polym. J.* **2003**, *35*, 911.
24. Wu, H.; Li, D.; Zhu, X.; Yang, C.; Liu, D.; Chen, X.; Song, Y.; Lu, L. *Electrochim. Acta* **2014**, *116*, 129.
25. Liu, L.; Chen, X. *Chem. Rev.* **2014**, *114*, 9890.
26. Zhang, X.; Ferraris, S.; Prenesti, E.; Verne, E. *Appl. Surf. Sci.* **2013**, *287*, 341.
27. Shin, J.; Samuelis, D.; Maier, J. *Adv. Funct. Mater.* **2011**, *21*, 3464.
28. Menéndez, R.; Alvarez, P.; Botas, C.; Nacimiento, F.; Alcántara, R.; Tirado, J.; Ortiz, G. *J. Power Sources* **2014**, *248*, 886.
29. Xiong, H.; Yildirim, H.; Shevchenko, E.; Prakapenka, V.; Koo, B.; Slater, M.; Balasubramanian, M.; Sankaranarayanan, S.; Greeley, J.; Tepavcevic, S.; Dimitrijevic, N.; Podsiadlo, P.; Johnson, C.; Rajh, T. *J. Phys. Chem. C* **2012**, *116*, 3181.